

Research Article

Development and Application of Equipment for Anchor Cable with C-Shaped Tube Tension-Shear Test System

Renliang Shan , Chen Liang, Weijun Liu , Yuzhao Jiang, and Tianwen Li

School of Mechanics and Civil Engineering, China University of Mining and Technology, Beijing 100083, China

Correspondence should be addressed to Weijun Liu; 1615541146@qq.com

Received 1 August 2022; Revised 21 September 2022; Accepted 17 October 2022; Published 2 November 2022

Academic Editor: Qiqing Wang

Copyright © 2022 Renliang Shan et al. This is an open access article distributed under the Creative Commons Attribution License, which permits unrestricted use, distribution, and reproduction in any medium, provided the original work is properly cited.

Based on the phenomenon of serious tensile-shear failure of bolts and cables, domestic and foreign scholars' research on the mechanical properties of bolts and cables has gradually changed from pure tensile to tensile-shear performance. To reduce the long-term bolt and cable breakage accidents in deep soft rock tunnels in coal mines, we independently developed a new type of support material—anchor cable with C-shaped tube and a corresponding tensile-shear test system. The system parameters are set through theoretical derivation, and the three main structures of the test system are designed with ANSYS: shear box, vertical loading reaction frame, and horizontal loading reaction frame. The numerical simulation results show that when the thickness of the shear box steel plate is 20 mm, the maximum strain is about 2.7‰. When the diameters of the vertical column and the horizontal bar are 220 mm and 80 mm, respectively, the maximum strains of the column and the horizontal bar are about 0.17‰ and 0.04‰, respectively. The strength and deformation of the three main structures meet the design requirements. The developed test system was tested on-site. The test results show that the system can perform tensile test and two different modes of the double shear test. The main structure has no obvious deformation during the test, meeting the design requirements. In addition, the rational design of the shear box eliminates the error caused by the shear block. The results show that the shear resistance of anchor cable with C-shaped tube is better than that of pure anchor cables. The research results can provide a reference for developing other similar test systems.

1. Introduction

With the rapid development of the coal industry, the engineering difficulty has parallelly escalated. For instance, given the tight construction period and other reasons, it is required to carry out mining or roadway excavation simultaneously in adjacent working faces [1]. Therefore, roadway support is an important link in coal mining. The purpose of roadway support is to ensure the stability of the surrounding rock, and that the surrounding rock does not undergo obvious deformation or even collapse and also the safety of operators [2–4]. After nearly 70 years of scientific research and practice in the field of coal mine roadway surrounding rock control by domestic and foreign experts [5–8], the bolt and anchor cable support in coal mines in China has become the most efficient and most commonly used support method. However, in the support process, the problem of

damage caused by the combined action of tension and shear has not been solved. Skrzypkowski et al. [9] found that the most severe areas where shear damage occurred in anchor rods and anchor cables were often due to faulting or relative slip of the surrounding rock. And the choice of support form near the fault was proposed. In order to enhance the shear resistance of the support material, Shan et al. [10–12] invented a new type of support material as shown in Figure 1, the combined tube and cable structure (hereafter referred to as ACC). This support material is supported by a combination of external C-shaped tube and internal anchor cable, which works synergistically. During the support process, due to the surrounding rock stress, the C-shaped tube gradually closes until it completely wraps the internal anchor cable and carries the load together with the anchor cable, which greatly improves the shear resistance of the support material.

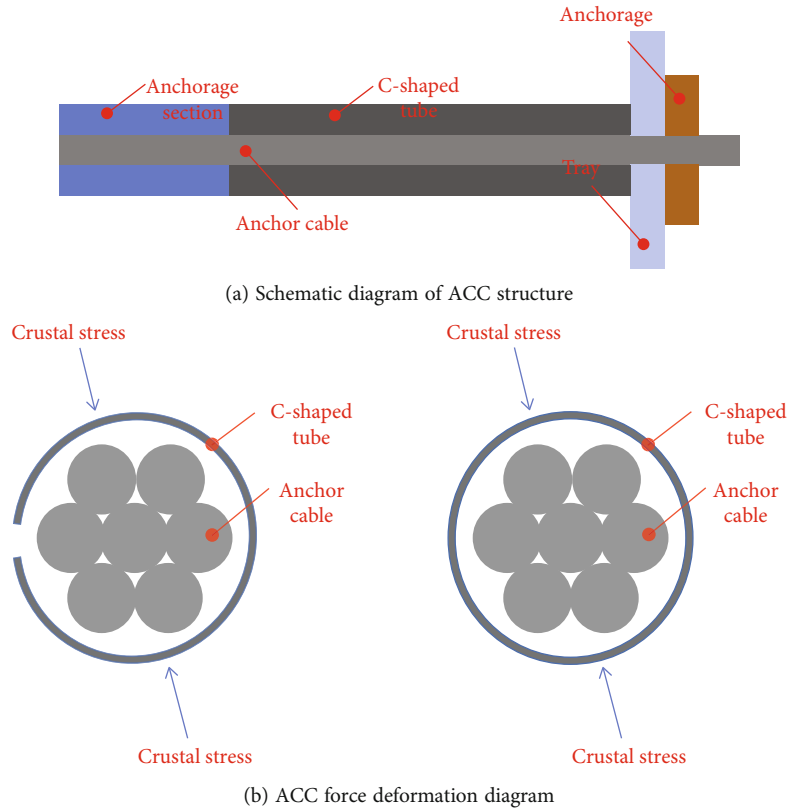


FIGURE 1: Schematic diagram of pipe and cable combination structure.

Aiming at the phenomenon of serious tensile-shear failure of bolts and cables, domestic and foreign scholars' research on the physical and mechanical properties of bolts and cables has gradually shifted from pure tension to tension-shear composite loads. To study the composite performance of tension and shear, scholars at home and abroad have developed or upgraded corresponding test systems and conducted related tests [3, 13]. Krzysztof found through his research that the most severe areas of shear damage in anchor rods and anchor cables are often caused by faulting or relative slip of the surrounding rock, while the surrounding rock stresses are often in the process of dynamic change [14]. The large deformation anchor cable tensile test system designed and developed by Zhigang et al. and He et al. [15, 16] is a self-developed through-center hydraulic group anchor tension system. The continuous tension test method is adopted to solve the problems of the large mass of the test system and the short range of the oil cylinder. Yang et al. [17] used this tensile test system to conduct tensile tests on anchor cables commonly used in domestic coal mines to study the relationship between ultimate tensile bearing capacity and cable diameter. Scholars at home and abroad mostly use electrohydraulic servo universal testing machines to perform tensile and shear tests on bolts and cables. The universal testing machine includes a test table, data acquisition, and servo control system. The data acquisition system is connected with the pressure, displacement, and deformation sensors for sampling to obtain the test data. Among them, Rasekh et al. [18] used the Instron testing machine to conduct shear tests on different types of bolts under dif-

ferent surrounding rock strengths and studied the interlayer shear and vertical displacement profiles. Jun et al. [19] used a universal testing machine to measure the bolt tensile and shear parameters and failure modes. Sheng-yi et al. [20] performed tensile and shear tests on GFRP bolts using an electrohydraulic servo universal testing machine. The test results show that the stress-strain curve of GFRP bolts is linear and has good deformation coordination with concrete. To measure the shear strength of bolts and cables more accurately, the double-sided shear test was proposed as a more effective test method [21, 22]. The double shear test machines used by most scholars are developed based on the earliest large shear frame, and most of them are composed of boxes, presses, pressure sensors, etc., that cannot only make mortar molds but also act as shear boxes. Among them, a pressure sensor needs to be arranged between the specimen and the anchor to measure the dynamic change of the preload force and the tensile force during the test. The pressure, displacement, and deformation sensors must be connected to the computer to collect and process the data [23, 24]. The double shear plane anchor rod and anchor cable tension-shear instrument developed by the University of Wollongong use steel molds to prevent concrete from collapsing during the test and can apply different pretightening forces to the anchor rod and anchor cable [25, 26]. Mirzaghobanali et al., Saadat and Taheri, Li et al., and Aziz et al. [25, 27–30] independently developed a new type of double shear device without contact between concretes. The original double shearing device MKIII is improved, and the friction between the contact surfaces of the concrete blocks is removed by installing a steel

groove bracket (U-shaped support) between two adjacent shear boxes to determine the preload pure shear strength of fully grouted bolts.

To sum up, domestic and foreign scholars have conducted experimental research on the tensile and shear properties of anchor cables from different angles in different ways, but they lack to provide a deep insight into the mechanical properties of ACC. As a new supporting material, ACC has the advantages of low cost, green, and environmental protection. It has been applied in many coal mines in Fenxi and other places in China, and the field application effect is good. Therefore, as a new material with wide application prospects, the research on its performance in the laboratory stage will be of great significance to the application of this support material in roadway support. To deeply study the physical and mechanical properties of ACC and anchor cables, the tensile and shear test system of anchor cable with C-shaped tube is developed by the existing laboratory tensile and shear test systems at home and abroad for reference. To test the physical and mechanical properties of anchor rods and cables more accurately, the system carries out a double shear plane test in shear test. There are two kinds of double shear tests: pure shear double shear test and shear plane compression shear composite load double shear test. Among them, the compression shear composite load on the shear plane refers to the compressive stress perpendicular to the shear plane applied by the anchor bolt and cable through the axial force during the test. Meanwhile, to resist the shear deformation, there is a shear stress parallel to the shear plane on the shear plane. Therefore, this double shear test mode is also known as the compression shear composite load double shear test on the shear plane. During the test, through some special means, the axial force of the anchor cable cannot apply compressive stress to the shear plane, and only the anchor cable can resist the slip of the shear plane through its bearing capacity. This double shear test is called pure shear double shear test. Since few articles introduce the design idea and research and development process of the test system in detail, this paper describes this part in detail, providing a reference for the research and development of similar systems. The new test system is used to test the anchor cable and ACC, verify the performance of the system, and obtain the shear performance of ACC.

2. Research on Test System

2.1. Design Ideas. Considering the insufficiency of the existing tensile and shear test systems for support members at home and abroad, to meet the requirements for testing their tensile and shear performance, a tensile and shear test system for anchor cable with C-shaped tube was developed. The new system is mainly improved in the following aspects: (1) solve the problem of insufficient loading space of the vertical shearing system. (2) Ensure that the shear box has sufficient bearing capacity and will not affect the test results due to the incompatibility with the shear surface. (3) The system can perform tensile and two different modes of double shear tests on supporting materials. The double shear test includes a pure shear test and shear plane compressive shear compos-

ite load shear test. (4) The method of acquiring and processing force and displacement data has been upgraded to improve test efficiency. The above aspects will be described in detail below.

Consider that the vertical shearing system of the existing part of the test equipment does not have enough loading space for the supporting members to be sheared. Therefore, the maximum displacement of the vertical shear system in the tensile-shear test system of the designed tube-cable composite structure is 250 mm; meanwhile, the maximum displacement of the horizontal tensile system is designed to be 200 mm. According to the size of the concrete blocks to be tested, the vertical loading space of the test system is 900 mm × 880 mm × 620 mm, and the horizontal loading space is 2000 mm × 520 mm × 400 mm.

The more mature double shear test systems in existing laboratories usually use metal shear boxes to prevent the blocks from disintegrating before the failure of the support members. Therefore, when designing the shear boxes, it is critical to ensure sufficient steel plate thickness first. Make the shear box have sufficient stiffness and strength to withstand the crushing force during the concrete block test. Meanwhile, since it is impossible to ensure that the concrete is fitted into the shear box during the test, it may cause the shear plane to be located inside the shear box unit. The axial force of the supporting member produces a lateral extrusion on the concrete block, causing the concrete block to compress laterally, which is smaller than the transverse dimension of the shear box. Both of these reasons will cause the shear box to shear the concrete block during the test and affect the test accuracy and results. Consequently, as shown in Figure 2, according to the side length of each concrete block 300 mm, the lateral dimension of each shear box unit is designed to be 295 mm, and a gap of 5 mm is reserved between the shear box units.

The tensile-shear test system of the combined structure of the tube and cable realizes the integration of the tensile testing machine and the double shear testing machine through the structural design of the vertical shear system and the horizontal tensile system. Among them, the pure shear state or the double shear test with the combined load of compression and shear on the shear plane can be selected according to the test needs. If the test is carried out under pure shear conditions, the friction between the shear surfaces can be reduced by applying lubricant, but the test accuracy cannot be guaranteed. Some researchers have also installed steel channel brackets between adjacent shear boxes to remove friction between the contact surfaces of concrete blocks. As shown in Figure 3, the tensile-shear test system of the tube-cable composite structure ensures that while the force is applied to the supporting member through the tensioning machine, the axial force of the supporting member is not transmitted to the shearing surface, thereby eliminating the friction between the structural surfaces. Therefore, tests satisfying pure shear conditions can be carried out.

In terms of data acquisition, to improve the test efficiency, the tensile and shear test system of the combined structure of tubes and cables uses servos in the lateral and

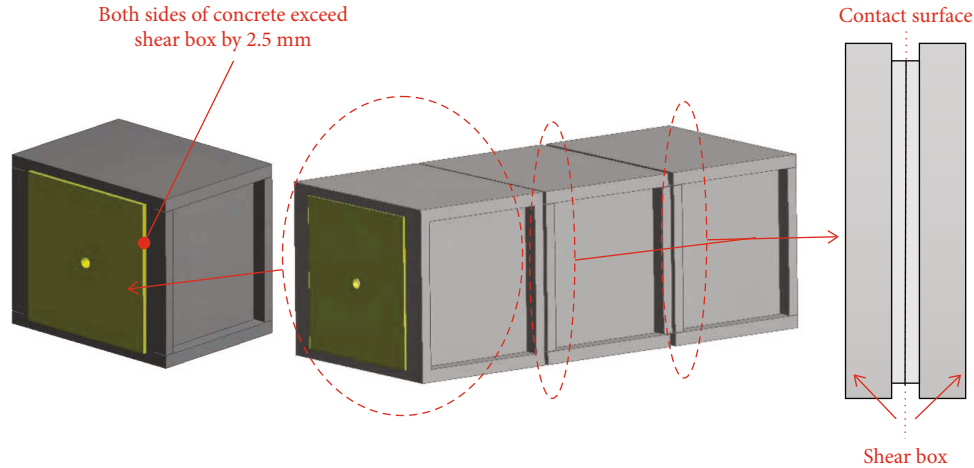


FIGURE 2: Schematic diagram of shear box structure.

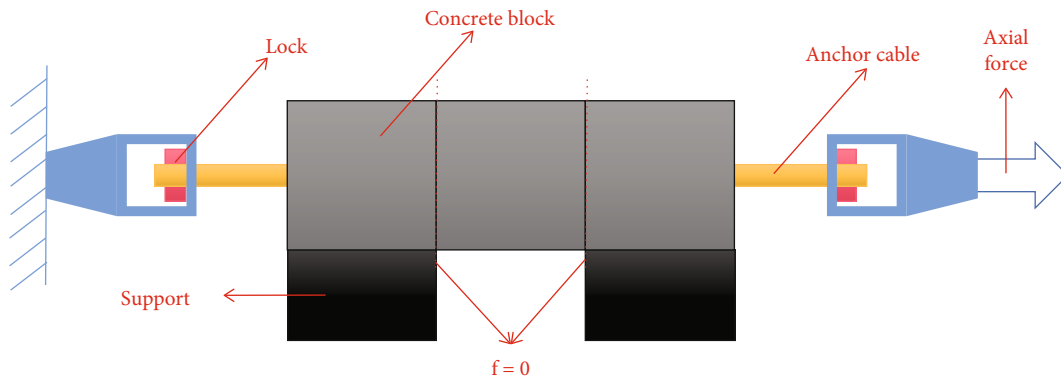


FIGURE 3: Schematic drawing of tensioning anchor cable.

axial directions to directly obtain the force and displacement data and integrate them into the self-developed software for unified processing. This article does not carry out the specific development of the system software part.

From the above aspects, China University of Mining and Technology (Beijing) designed and constructed a tensile-shear test system for tube-cable composite structures.

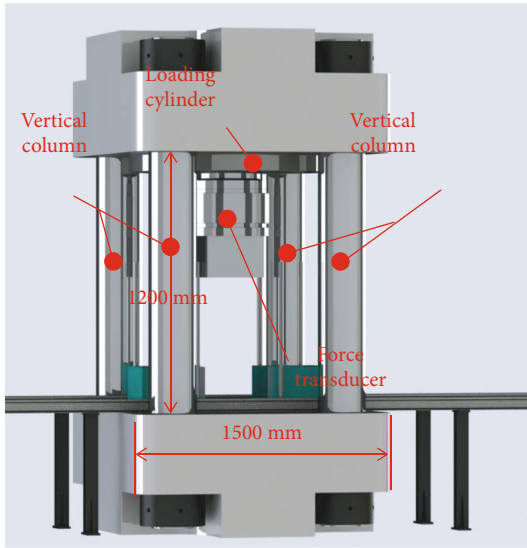
2.2. Composition of the Test System. The tube and cable combined structure test system is mainly composed of a main testing machine, servo hydraulic system, measurement control system, etc. Among them, the main testing machine is shown in Figure 4, consisting of a vertical shearing system and a horizontal stretching system. Both the vertical and horizontal main testing machines are equipped with servo loading cylinders to provide power for loading, to realize shear and tensile tests of supporting members. Moreover, install a load measurement sensor and displacement sensor to directly obtain vertical and horizontal force and displacement data. The motor drives the horizontal mainframe to move back and forth on the track. At the beginning of the test, move the horizontal mainframe to the side of the vertical mainframe, and the vertical shearing and horizontal tensile tests can be carried out simultaneously.

The shear box, also known as the specimen loading box, is an important component that restrains the cracking of concrete blocks and bears the shear load in the vertical direction, as shown in Figure 5. To facilitate the installation and removal of concrete blocks before and after the test, the plates are connected by bolts. Three shear box units are installed with a concrete block as a group for shear test. During the test, the shear box units on both sides were placed in the support centers on both sides of the vertical shearing system, and the shear box units in the middle were suspended in the air to be sheared.

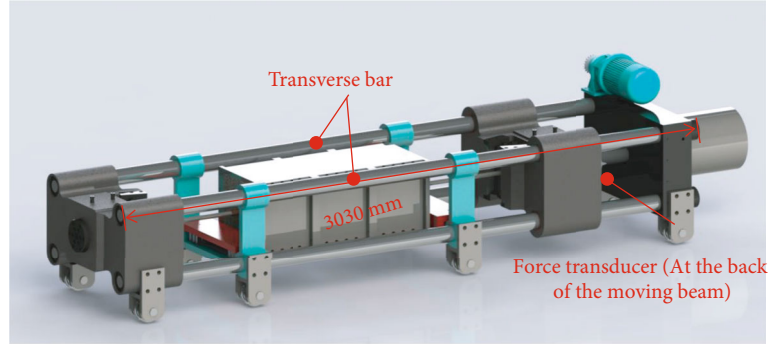
2.3. Test System Parameters

2.3.1. Horizontal Loading System Parameters. The horizontal loading system in the tensile-shear test system of the tube-cable composite structure mainly conducts tensile tests on the bolt, anchor cable, and ACC. The following will design the parameters of the horizontal loading system:

- (1) Determine the maximum test load of the horizontal loading system. The $\Phi 21.8$ mm anchor cable and the ACC combined with the $\Phi 21.8$ mm anchor cable and the C-shaped tube are the supporting components that are used more frequently and have better



(a) Vertical shear system



(b) Horizontal stretching system

FIGURE 4: Main test system.

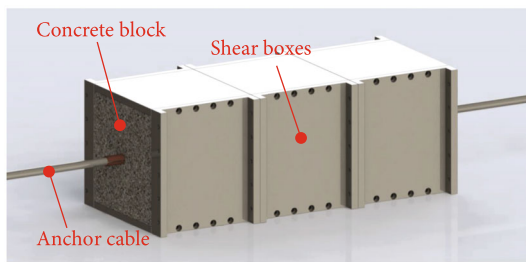


FIGURE 5: Shear box.

supporting effects at the current stage, so they become the focus of laboratory research. However, with the development of roadway support technology, the application of large-diameter anchor cables will become more extensive, and the mechanical properties of anchor cables will be significantly improved in the future. Considering the long-term practicability of the system, when designing the loading parameters of the tensile-shear test system for the combined structure of the tube and cable, the design is based on the maximum tensile force when the $\Phi 28.6$ mm anchor cable fails. According to market research, the maximum tensile force of $\Phi 28.6$ mm anchor cable is about 1000 kN. Based on safety considerations, the safety factor is taken as 1.2, and the design value of the maximum test load of the horizontal loading system is finally determined to be 1200 kN

- (2) Determine the maximum test displacement of the horizontal loading system. During the test, a support member with a length of 2 m or less is generally used for the test. Herein, the 2 m anchor cable is used for calculation. The elongation rate of a mine anchor cable is generally 5%. Based on safety considerations, this paper calculates with 8%. Then, the maximum

displacement of the horizontal pulling system is as follows:

$$l_{\max} = 2000 \times 0.08 = 160 \text{ mm.} \quad (1)$$

Taking the safety factor of 1.25, the design value of the maximum displacement of the horizontal loading system is 200 mm.

2.3.2. Parameters of Vertical Loading System. The vertical loading system in the tube-cable composite structure test system is to study the shear resistance of the bolt and cable and the ACC. According to the mechanical analysis, the ACC should have a more prominent shear resistance than the bolt and cable. The maximum shear force to be subjected is calculated as a reference for the design value of the vertical loading system test load. The ACC comprises an inner anchor cable and an outer C-shaped tube. The maximum shear force of the ACC that can provide to the shear plane is the “pin effect” of the anchor cable and the C-shaped tube to resist shear deformation and the concrete masonry during the test. The sum of the frictional reaction forces at the contact surfaces between the blocks. Among them, the C-shaped tube and anchor cable made of Q345b steel are mostly used for support at the current stage. However, because the C-shaped tube is an important part of the supporting member, its materials are widely used, and there is room for improvement in strength. Therefore, when calculating the design value of the test load of the vertical loading system in this paper, the design is firstly carried out by taking the $\Phi 21.8$ mm anchor cable and 431 stainless steel C-shaped tube that are used more and has a higher tensile strength at the construction site as an example. Based on safety considerations and comprehensive market research, the maximum tensile force that the $\Phi 21.8$ mm anchor cable can bear is 700 kN, and the tensile strength of 431 stainless steel

TABLE 1: Composition and main technical parameters of the tensile and shear test system of the combined pipe and cable structure.

System composition	Technical parameter	Ranges
Vertical loading system	Maximum test load (kN)	6000
	Maximum displacement (mm)	250
	Loading rate (mm/min)	0-100
Horizontal loading system	Maximum test load (kN)	1200
	Maximum displacement (mm)	200
	Loading rate (mm/min)	0-100
Specimen	Diameter Φ (mm)	15-33
	Length (mm)	2000
Block loading box $\times 1$	Block size (mm)	$300 \times 300 \times 300$
Block sample box $\times 3$	Block size (mm)	$300 \times 300 \times 300$
Hydraulic system	Fixed work stress (MPa)	28
	Servo loading cylinder rated working pressure (MPa)	21
	Vertical system cylinder maximum output value (kN)	6000
	Maximum output value of horizontal system cylinder (kN)	1200
Measurement control systems	Vertical loading system force transducer range (kN)	6000
	Horizontal loading system force sensor range (kN)	1200
	Force sensor accuracy	0.2% FS
	Vertical loading system displacement sensor range (mm)	250
	Horizontal loading system displacement sensor range (mm)	200
	Displacement sensor accuracy	0.2% FS

is 1900 MPa. The three-part shear bearing capacity provided by the ACC to the shear plane will be calculated step by step.

- (1) Consider the “pin effect” of the anchor cable itself against deformation. According to Tresca guidelines, when a material is subjected to simple tension, the pure shear yield stress is half of the simple tensile yield stress, namely,

$$\tau_{0m} = \frac{1}{2} \sigma_{0m}, \quad (2)$$

where τ_{0m} is the pure shear yield stress of the anchor cable and σ_{0m} is the tensile yield stress of the anchor cable.

From the above, the maximum tension that the 21.8 mm anchor cable can bear is 700 kN, so we can get

$$F_{0m} = (\sigma_{0m} \times s_{0m}) = 700 \text{ kN}, \quad (3)$$

where F_{0m} is the maximum tension of the anchor cable and s_{0m} is the cross-sectional area of the anchor cable.

According to the Tresca criterion, the maximum “dowel effect” force that the anchor cable can provide when sliding in the single shear plane is

$$T_{0m} = \tau_{0m} \times s_m = \frac{1}{2} (\sigma_{0m} \times s_m) = 350 \text{ kN}. \quad (4)$$

TABLE 2: Main parameters of structural steel.

Material	Density (kg/m ³)	Elastic modulus (MPa)	Poisson's ratio	Allowable stress (MPa)
Structural steel	7850	2.1×10^4	0.3	113

Since the test system carries out double shear test, that is, there are two shear planes, the maximum shear force provided by “dowel effect” in the process of double shear test is twice that of single shear, that is

$$T'_{0m} = 2T_{0m} = 700 \text{ kN} \quad (5)$$

- (2) Consider the “dowel effect” of a C-shaped tube to resist shear deformation. It is known that the tensile strength of 431 stainless steel is 1900 MPa, the outer diameter of a C-shaped tube is 28 mm, and the inner diameter is 24 mm. Through calculation, the maximum tensile force when a C-shaped tube is damaged is

$$F_{0C} = \sigma_C \times s_C = 310.23 \text{ kN}, \quad (6)$$

where F_{0C} is the maximum tensile force of C-shaped tube, σ_C is the tensile yield stress of the C-shaped tube, and s_C is the cross-sectional area of C-shaped tube.

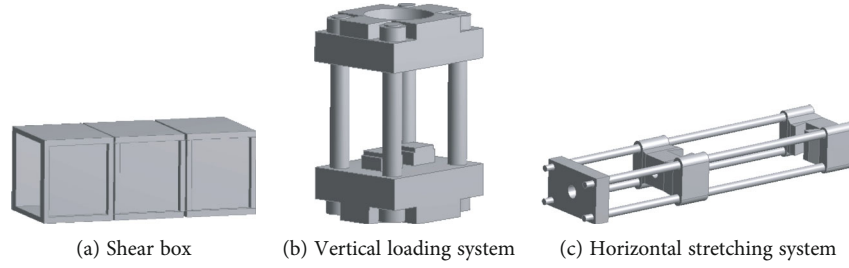


FIGURE 6: Main structure model of a test system.

Similar to the anchor cable, we believe that the C-shaped tube meets the Tresca criterion, and the maximum “dowel effect” force that the C-shaped tube can provide during the test is as follows:

$$T_C = 2 \times \tau_C \times s_C = 2 \times \frac{1}{2} (\sigma_C \times s_C) = 310.23 \text{ kN}, \quad (7)$$

where T_C is the maximum “pin” force that a C-shaped tube can provide and τ_C is the pure shear yield stress of a C-shaped tube

- (3) Frictional reaction: in the double shear test, there is not only the “pin effect” of support components. To restrain the relative slip of the shear plane, the normal stress of the support member acting on the shear plane will also produce a friction reaction parallel to the shear plane. It is generally considered that the calculation of the friction reaction meets the Mohr-Coulomb criterion:

$$\tau_n = c + \sigma_n \tan \phi. \quad (8)$$

The resultant frictional reaction force is thus calculated:

$$T_n = \tau_n \times s_n = c \times s_n + \sigma_n s_n \tan \phi, \quad (9)$$

where τ_n is the friction reaction force, σ_n is the normal stress of the support member acting on the shear plane, c is the cohesion of the shear plane, s_n is the area of the shear plane, ϕ is the friction angle in the shear plane, and $\sigma_n s_n$ is the axial force exerted by the supporting member on the concrete block, that is, F_{0m} . The value range of friction angle and cohesion in rock mass is large. Based on safety considerations, it is taken as 60° and 15 MPa in the calculation. According to formula (3) and formula (9), the friction reaction is $T_n = 2562.44 \text{ kN}$.

To sum up, ACC composed of 21.8 mm anchor cable with a C-shaped tube is tested; the system needs to provide the maximum vertical load:

$$T_1 = T_0 + T_n = T'_{0m} + T_C + T_n = 3572.67. \quad (10)$$

Consider that some support sites gradually began to use anchor cables with a diameter of $\Phi 28.6 \text{ mm}$ for support. To ensure the practicability of the cable pole tension shear test system for a long-term test, the maximum vertical load value

of ACC formed by the combination of anchor cable with a diameter of 28.6 mm and an external C-shaped tube is calculated during the test. Because the calculation process is consistent with $\Phi 21.8 \text{ mm}$, ACC is the same, so it will not be repeated, and only the final calculation result is given as $T_2 = 4463.9 \text{ kN}$. Based on safety considerations, if the safety factor is taken as 1.3, the maximum test load of the required vertical system is 5803 kN. According to the optional output value of the servo cylinder, the design value of the maximum test load in the vertical direction is 6000 kN

In the design idea of Section 2.1 of this paper, the design value of the maximum displacement of the vertical loading system is determined to be 250 mm. Its purpose is to provide enough loading space to make the supporting members cut during the test. This part will not be repeated in this section.

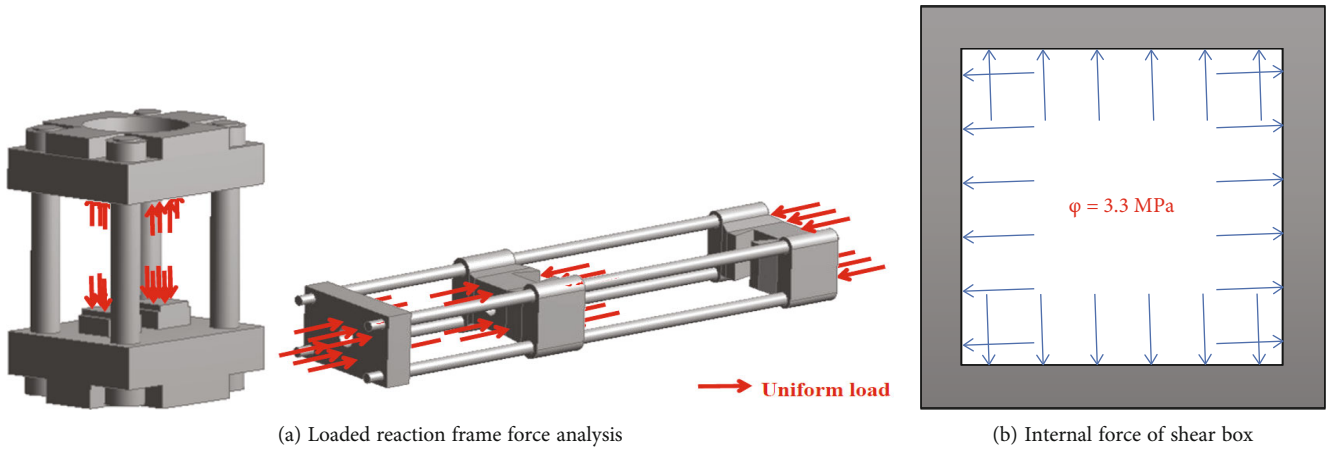
2.3.3. Other System Parameters. According to the relevant literature on the existing domestic and foreign support member tensile and shear test systems, the block size is determined to be $300 \text{ mm} \times 300 \text{ mm} \times 300 \text{ mm}$. According to the block size, the main structure size and main technical parameters of the test system are determined. The specific parameters are listed in Table 1. The maximum tensile force that the $\Phi 21.8 \text{ mm}$ anchor cable can bear is 700 kN. So, it can be obtained.

3. Structural Analysis

If the structural strength and deformation of the test system do not meet the design requirements, it will greatly impact the test results and even damage the equipment. The ANSYS Workbench work platform is designed to be a collaborative simulation environment and has advantages in structural static analysis of complex mechanical systems. Therefore, in this section, the ANSYS Workbench is used to perform static analysis on the shear box and the two reaction frames, determine the thickness of the shear box steel plate and the column diameter of the reaction frame, and analyze whether the structure of the equipment meets the structural design requirements.

3.1. Model Establishment and Mesh Division. The main structure model of the tube-cable (rod) tensile-shear test system is established, the selected material is structural steel, and the material parameters are listed in Table 2.

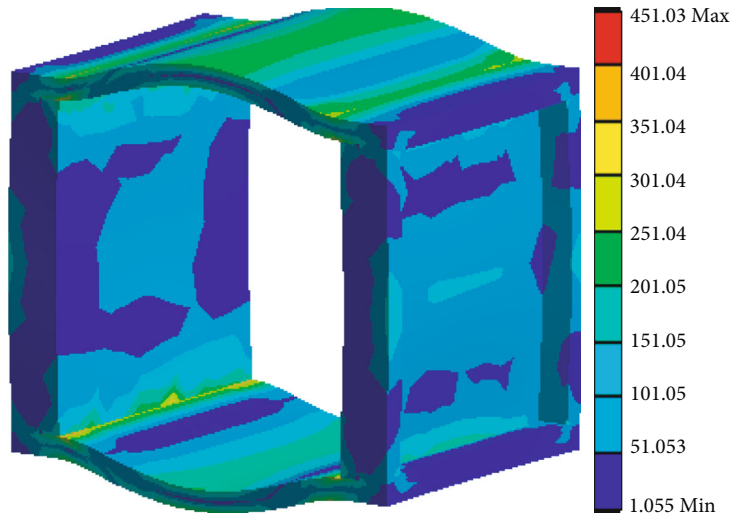
Simplify structural models during model building. Among them, the combination method between the shear box steel plate and the steel plate is simplified from the bolt



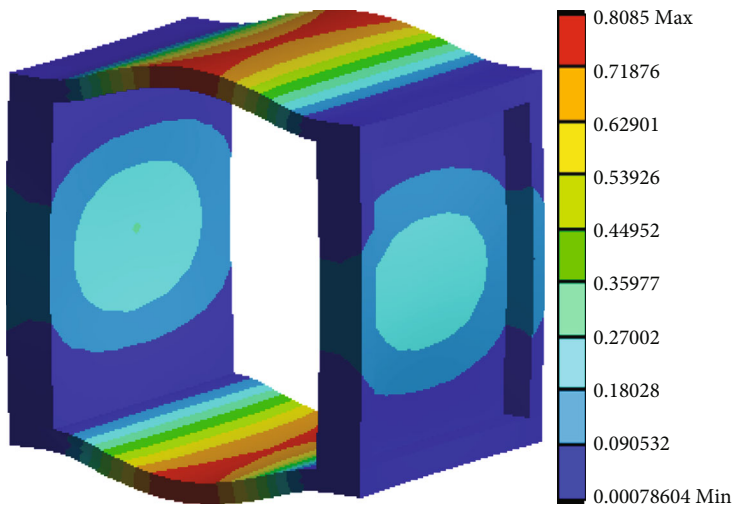
(a) Loaded reaction frame force analysis

(b) Internal force of shear box

FIGURE 7: Schematic diagram of the main structure under force.

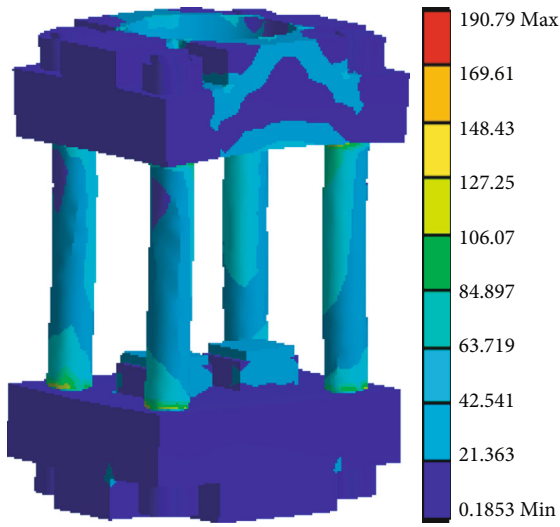


(a) Equivalent stress distribution contour of the shear box element

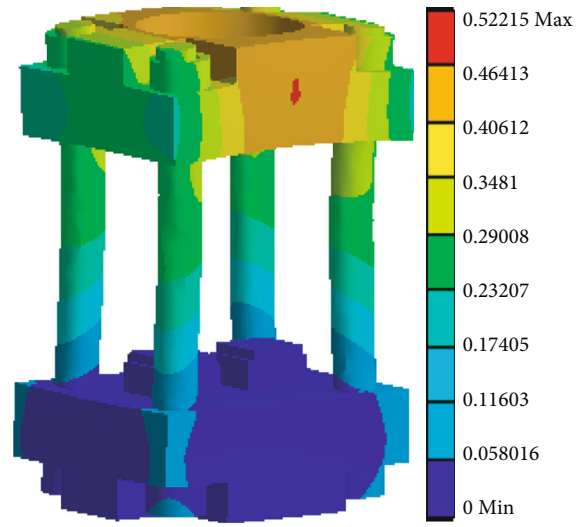


(b) Shear box element deformation distribution cloud map

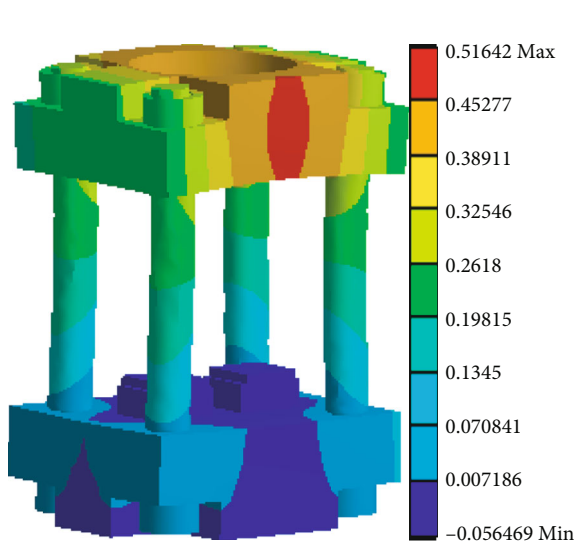
FIGURE 8: Numerical simulation of shear box element.



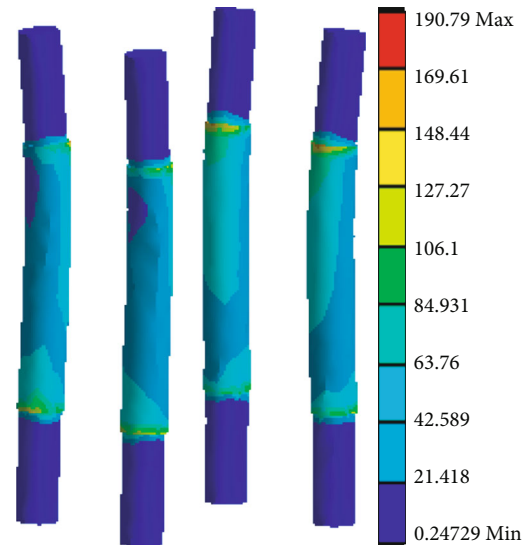
(a) Equivalent stress distribution cloud map of a vertical system



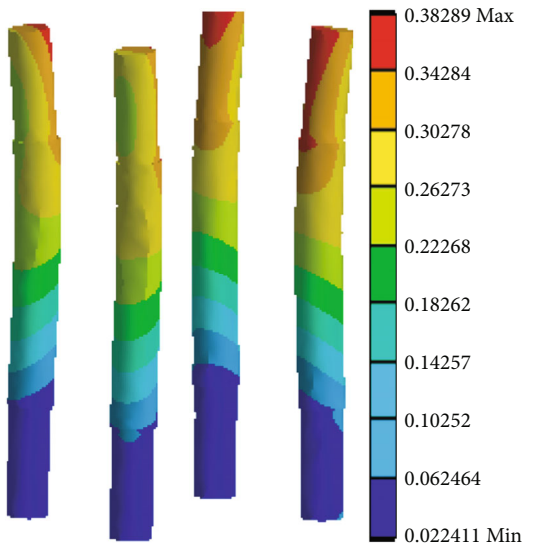
(b) Distribution cloud map of total deformation of a vertical system



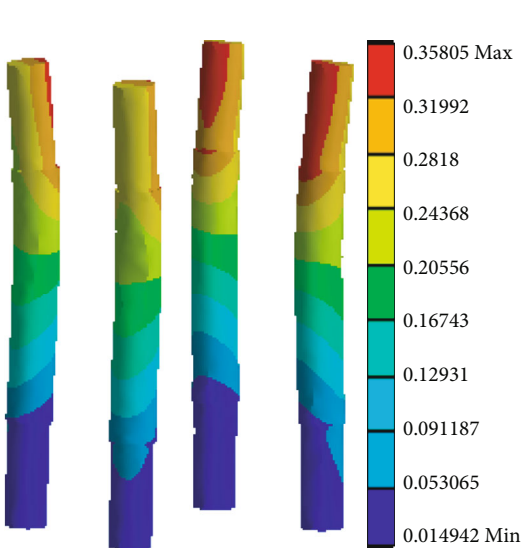
(c) Axial deformation distribution cloud map of a vertical system



(d) Equivalent stress distribution cloud diagram of a vertical column

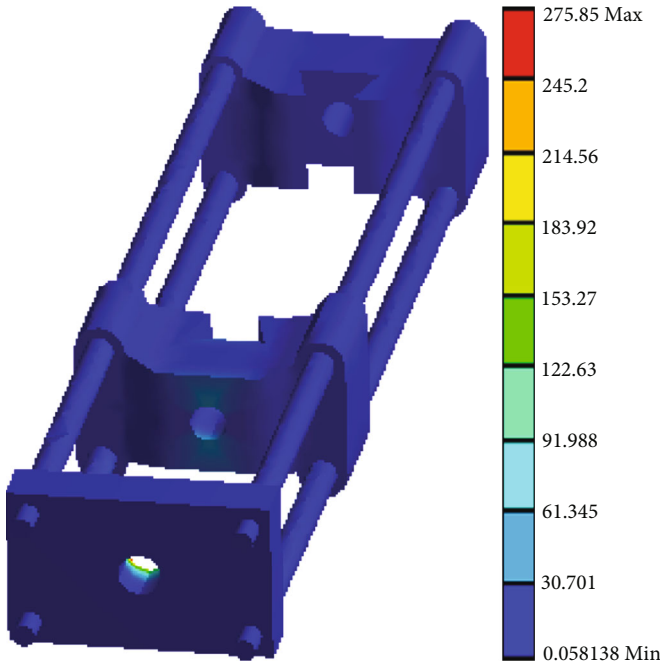


(e) Distribution cloud map of total deformation of a vertical column

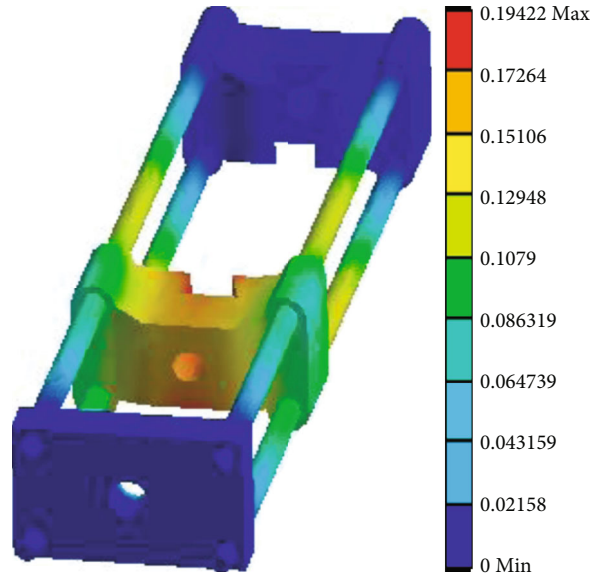


(f) Axial deformation distribution cloud map of a vertical column

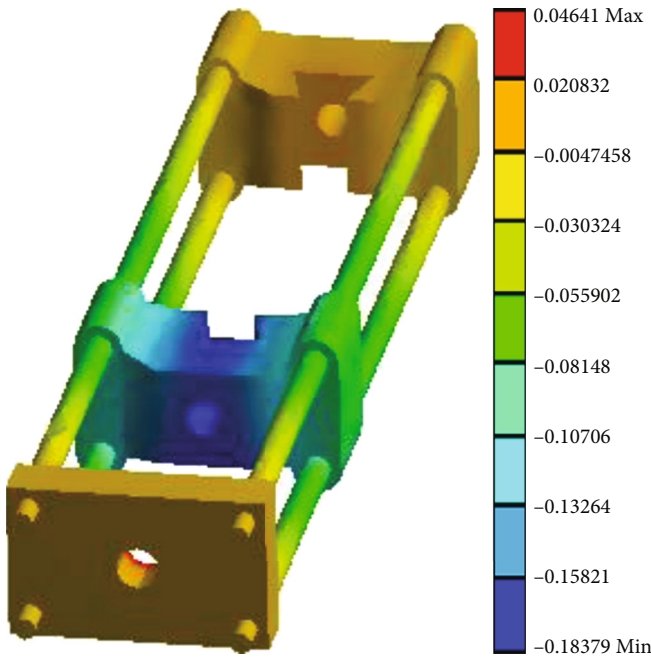
FIGURE 9: Numerical simulation results of vertical shear system.



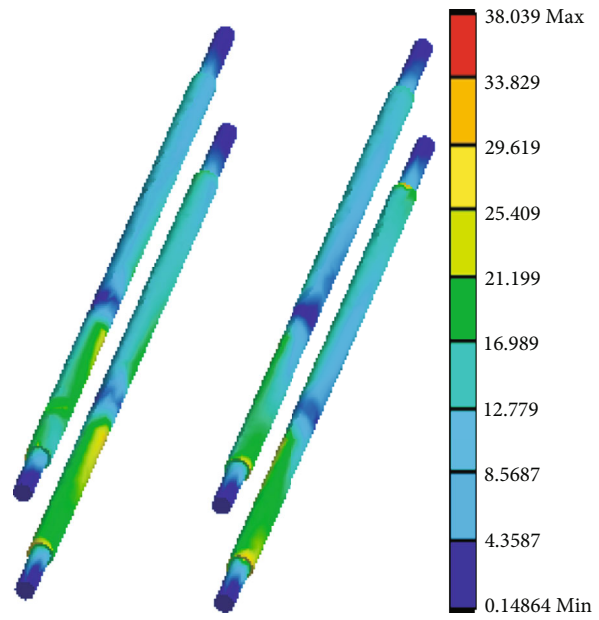
(a) Equivalent stress distribution cloud diagram of tensile system



(b) Total deformation distribution cloud map of tensile system

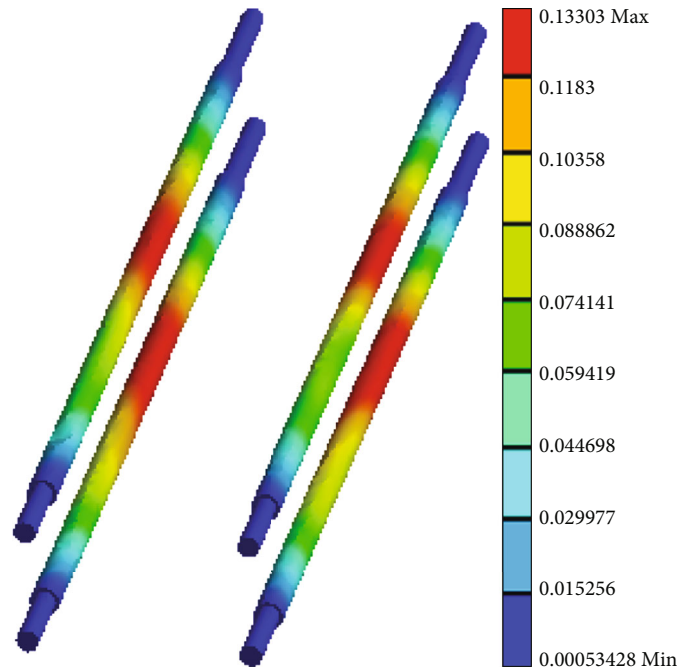


(c) Axial deformation distribution cloud map of tensile system

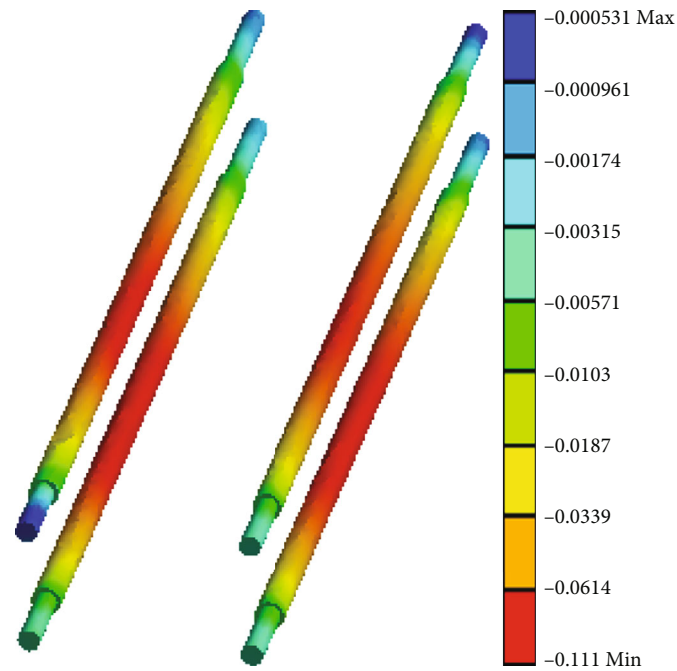


(d) Equivalent stress distribution cloud map of the horizontal column

FIGURE 10: Continued.



(e) Cloud map of total deformation distribution of the horizontal column



(f) Axial deformation distribution cloud map of the horizontal column

FIGURE 10: Numerical simulation results of the horizontal tensile system.

connection to the binding contact in the ANSYS Workbench environment. The vertical loading reaction frame and the horizontal loading reaction frame ignore components, such as bolts that have little influence on the stiffness and strength of the system, and set the connection between the column and the base and between the horizontal crossbar and the end plate as binding contact. Moreover, ignore the small structures such as the transition arcs and grooves between

the end plate and the base. The simplified model is shown in Figure 6.

3.2. *Static Analysis.* Since there are no relevant design standards for the research and development of tensile-shear test system equipment at home and abroad, based on safety considerations, this paper proposes the following design standards for the main structure and shear box of the

tube-cable composite structure tensile-shear test system: the main structure frame and shear box are required. The deformation of the cutting box is less than 1 mm. The shear box strain should be within 3‰, and the frame strain should be within 0.3‰. Among them, the strength of the shear box must be less than the yield strength of the selected high-strength steel plate (460 MPa), and the strength of the main structure frame must be less than the strength of the selected steel (690 MPa). Given the above requirements, the static analysis of the main structure of the test system and the shear box is conducted. Among them, the vertical loading counterforce frame, horizontal loading counterforce frame, and shear box are subjected to the forces shown in Figure 7.

3.2.1. Shear Box. As shown in Figure 7, due to the expansion of the concrete block inside the shear box unit during the double shear test, a large force is generated on the inner surface of the shear box unit. Given the lack of relevant literature at home and abroad as a reference, based on safety considerations, the shear box is regarded as a pressure vessel under a uniform load, and the stress on the inner surface of the shear box under a uniform load of 3.3 MPa (300 kN on each surface) is analyzed. The wall thickness of the steel plate was revised and verified repeatedly, and finally, the wall thickness of the steel plate was determined to be 20 mm.

Figure 8 shows the nephogram of the equivalent stress distribution and total deformation of the shear box of the steel plate with a wall thickness of 20 mm. As shown in Figure 8, the upper and lower side plates of the shear box are slightly bent and deformed, and the maximum deformation is about 0.81 mm, which occurs in the middle of the upper and lower side plates. The maximum deformation part is funnel-shaped, and the calculated strain is about 2.7‰, less than 3‰. The maximum stress of the shear box is 451.03 MPa, less than the yield strength of the high-strength steel plate, which is 460 MPa, and no damage occurs. The maximum stress occurs at the connection between the shear box surface and the surface, which is the phenomenon of stress concentration caused by the sudden change in structure. Except for the surface connection, the overall stress of the shear box is kept below 300 MPa.

3.2.2. Vertically Loaded Reaction Frame. Based on safety considerations, the overall strain of the designed vertical loading reaction frame is required to be within 0.3‰. According to the numerical simulation results, the column diameter of the vertical loading reaction frame is repeatedly corrected and finally determined to be 220 mm. The static analysis of the structure is now carried out.

Since a servo cylinder with a maximum load of 6000 kN is used in the vertical direction of the tensile and shear test system of the tube-cable composite structure, a load of 6000 kN is applied to the vertically loaded reaction frame, and the bottom surface of the reaction frame is restrained in the three directions, i.e., x , y , and z displacements.

The equivalent stress distribution and deformation cloud maps of the vertical frame are shown in Figures 9(a)–9(c). The results show that the maximum stress of the whole

TABLE 3: Double shear test scheme.

Program	Component type	Anchor type	Preload (kN)
Z1	ACC	1 × 19 strands Φ21.8 mm	10
Z2	ACC	1 × 7 strands Φ21.6 mm	250
Z3	ACC	1 × 7 strands Φ21.6 mm	10
Z4	ACC	1 × 19 strands Φ21.8 mm	250
Z5	Anchor cable	1 × 7 strands Φ21.6 mm	250
Z6	Anchor cable	1 × 19 strands Φ21.8 mm	250

frame is about 190.79 MPa, which is less than the yield strength of 690 MPa, and the strength meets the requirements. The maximum deformation is about 0.52 mm, the axial deformation is about 0.57 mm, and the deformation is less than 1 mm, which is within the design allowable range. Among them, the force of the four columns in the vertical loading reaction frame is analyzed separately, and the equivalent stress distribution cloud map and deformation cloud map of each column are shown in Figures 9(d)–9(f). The results show that due to the symmetry of the structure, the deformation of the four columns is similar, the deformation characteristic of each column is axial stretching, and the middle of each column is bent toward the center of the structure. The maximum deformation of about 0.38 mm is located inside the top of each column, the axial deformation is about 0.34 mm, and the deformation of the column is less than 1 mm. The calculated total strain is about 0.17‰, less than 3‰, within the allowable range. The maximum stress of about 190.79 MPa is at the connection between the column, the reaction beam, and the lower base. The main body stress of the four columns is in the range of 20–80 MPa, which is less than the yield strength of 690 MPa, and the strength meets the design requirements.

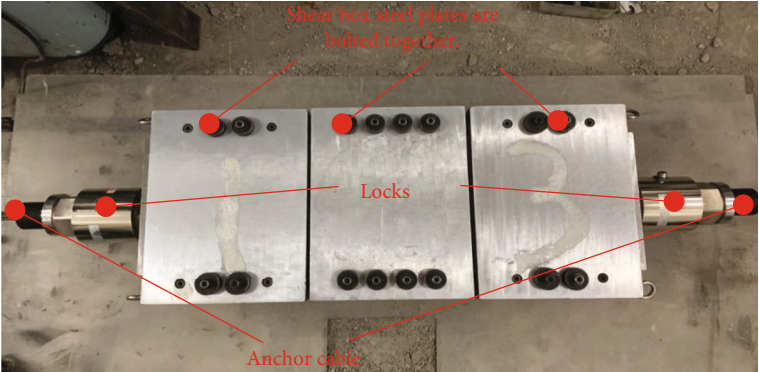
3.2.3. Horizontal Loading Reaction Frame. Based on safety considerations, the overall strain of the designed horizontal loading reaction frame is required to be within 0.3‰. According to the numerical simulation results, the column diameter of the horizontal loading reaction frame was repeatedly corrected and finally determined to be 80 mm. Now the static analysis of the structure is conducted.

Simulate the stress state of the horizontal reaction frame when the horizontal servo cylinder is loaded to the maximum load of 1200 kN. The equivalent stress distribution cloud diagram and deformation cloud diagram of the horizontal reaction frame are shown in Figures 10(a)–10(c).

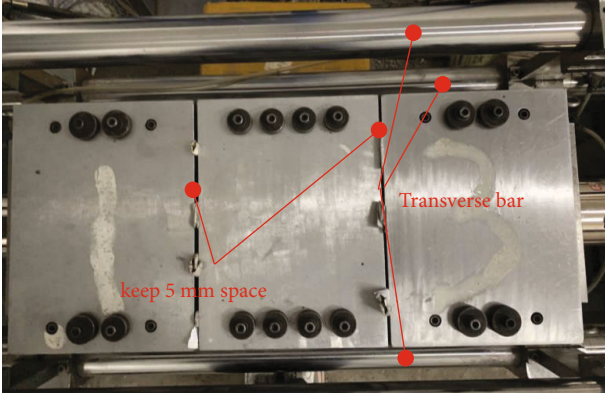
The results show that the center of the end plate of the horizontal frame in the hole is reserved for the anchor cable and the ACC, so the phenomenon of stress concentration occurs. The maximum stress of the frame which occurs here is about 275.85 MPa, the maximum stress is less than the yield strength of the steel used in the column 690 MPa, and the main structural stress of the frame is below 30 MPa, meeting the strength design requirements. The



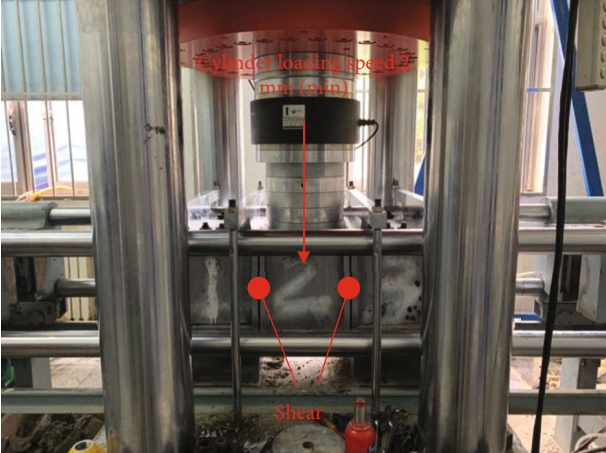
(a) Uniaxial compressive strength test



(b) Installation of equipment and blocks



(c) The shear box is placed in the horizontal loading space



(d) Conduct double shear test

FIGURE 11: Continued.



(e) Analyze at the end of the test

FIGURE 11: Test procedure.

maximum deformation of the frame is about 0.19 mm, and the calculated strain is about 0.06‰. The axial deformation is about 0.22 mm, and the deformation is less than 1 mm, meeting the deformation design requirements. Among them, the stress situation of the four transverse rods in the horizontal loading reaction frame is analyzed separately, and the equivalent stress distribution cloud diagram and deformation cloud diagram of the four transverse rods are shown in Figures 10(d)–10(f). The deformation of the crossbars is similar. The maximum deformation of each crossbar is about 0.13 mm, which occurs in the middle of the crossbar. Between the fixed beam and the movable beam, the axial deformation is about 0.11 mm, and the deformation is less than 1 mm. The calculated total strain is about 0.04‰, which is less than 0.3‰, and the results show that the deformation of the structure is within the allowable range. The maximum stress of the horizontal bar is about 38.04 MPa, which is at the splicing point between the column and the fixed beam. The main stress of the four horizontal bars is below 15 MPa, which is far less than the steel yield strength, which is 690 MPa, and the strength meets the design requirements.

4. System Test

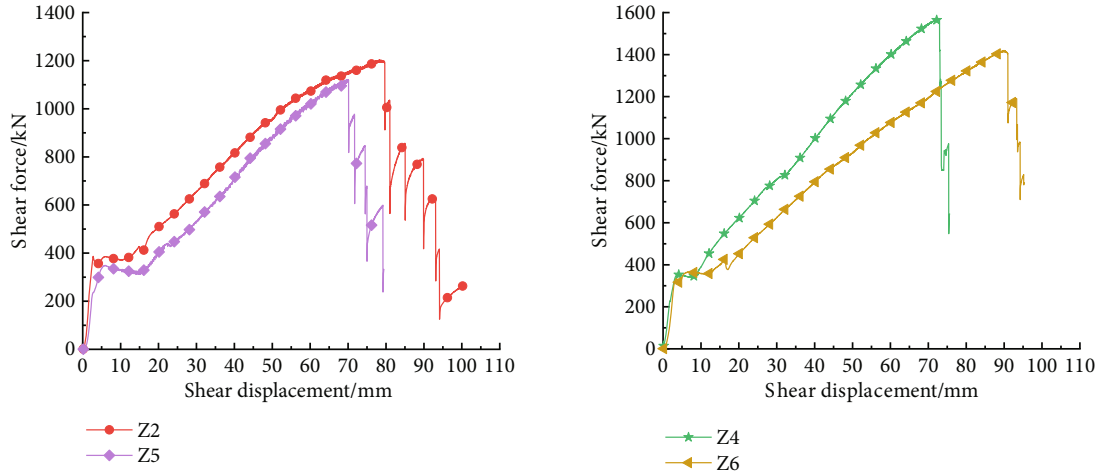
The double shear test of the ACC and the anchor cable is carried out by applying the tensile-shear test system of the combined structure of the tube and cable. Whether the test system can be successfully tested is verified, and the practicability and accuracy of the test system are analyzed according to the test results.

4.1. Double Shear Test. The main purpose of the test is to verify the feasibility of the tensile-shear test system of the tube-cable composite structure and to study the influence of the three factors of member type, anchor cable type, and pretightening force on the shear performance of the supporting member through the test. Considering the construction site of roadway support, in order to suppress roadway deformation and delamination and prevent damage to the

surrounding rock, a certain size of prestress is often applied to anchor rods and anchor cables to improve the surrounding rock conditions and enhance the support effect. In order to further analyze the mechanical behavior of anchor ropes and ACC in actual projects, the prestressing force is also analyzed as one of the factors affecting its shear performance in the indoor test. The specific test plan is listed in Table 3.

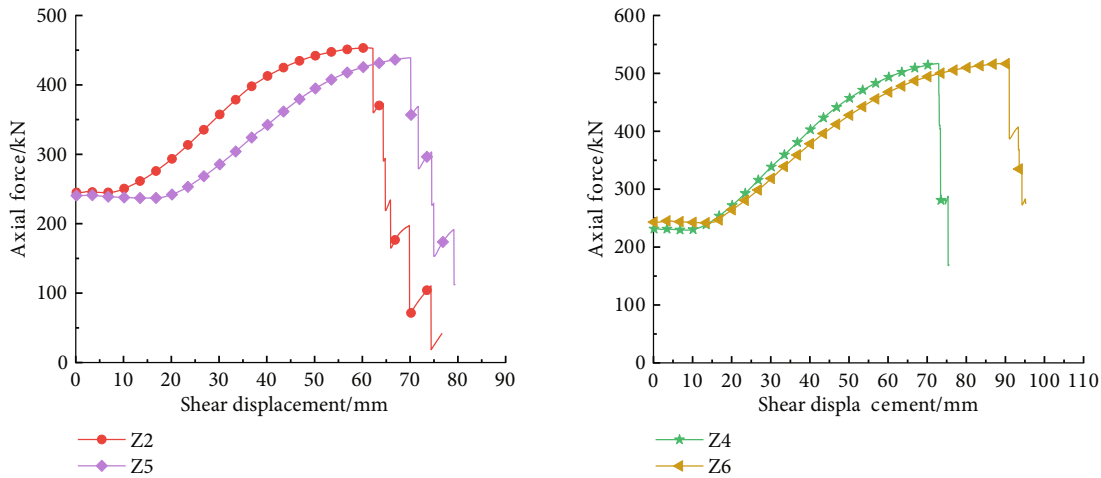
The uniaxial tensile capacity of the test anchor cable of $\Phi 21.8$ mm is 596 kN, and the pure tensile capacity of the test C-shaped tube is 105 kN, which is made of Q345b steel with a tensile strength of 630 MPa. The maximum pure shear force that the anchor cable can withstand is 1192 kN, and the maximum pure shear force that the C-shaped pipe can withstand is 210 kN.

The test process is as follows: first make blocks in the laboratory, then remove the formwork after curing in the curing room for one day, and then continue curing for 27 days to conduct the test. The uniaxial compressive strength test of small blocks of 100 mm \times 100 mm \times 100 mm was carried out, and the average compressive strength of concrete blocks was measured to be 38.12 MPa. Install blocks, sensors and other equipment, and support members, and apply pretightening force to the support members. After completing the preparations, place the shear box in the center of the specimen support plate of the horizontal tensile system. Move the horizontal mainframe to one side of the vertical mainframe to ensure that the vertical shear load is only applied to the center of the central shear box element. During the test, the central shear box and block will be loaded in the air. To prevent the shear box and block from turning over when the normal load is applied, fixed beams and fixed rods are added on both sides of the upper part of the shear box unit. During the test, the shear box and block in the middle were loaded at a rate of 2 mm/min, and the support members were sheared, causing relative slippage on the shear plane until the support members broke to end the test. After the test, remove the beam and remove the vertical load. Remove and observe the cracks of concrete blocks and the fracture mode and fracture of supporting specimens, and



(a) Comparison of $\Phi 21.6$ mm ACC and $\Phi 21.6$ mm anchor cable (b) Comparison of $\Phi 21.8$ mm ACC and $\Phi 21.8$ mm anchor cable

FIGURE 12: Comparison of shear resistance of different supporting materials.



(a) Comparison of $\Phi 21.6$ mm ACC and $\Phi 21.6$ mm anchor cable (b) Comparison of $\Phi 21.8$ mm ACC and $\Phi 21.8$ mm anchor cable

FIGURE 13: Comparison of axial force differences of support component types.

TABLE4: A comparison of the axial bearing performance of supporting members.

Test group	Support type	Axial force at break (kN)	Axial bearing capacity increase percentage
A	$\Phi 21.6$ mm ACC	453.54	3.3%
	$\Phi 21.6$ mm anchor cable	439.09	
B	$\Phi 21.8$ mm ACC	517.06	0%
	$\Phi 21.8$ mm anchor cable	517.06	

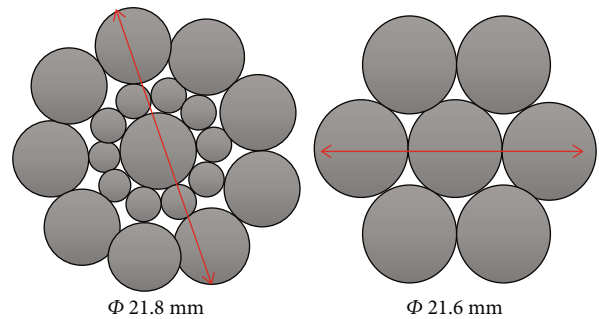


FIGURE 14: Anchor cable structure.

analyze the test results according to the test data. The main procedure of the test is shown in Figure 11.

4.2. System Verification. During the test, observe the relative position of the shear box and the concrete block. Since a

5 mm gap is set between the shear box units and the transverse dimension of the shear box is smaller than the transverse dimension of the concrete block, during the test, the shear plane is always located in the gap between the shear box units and the shear box. The relative slip of the contact

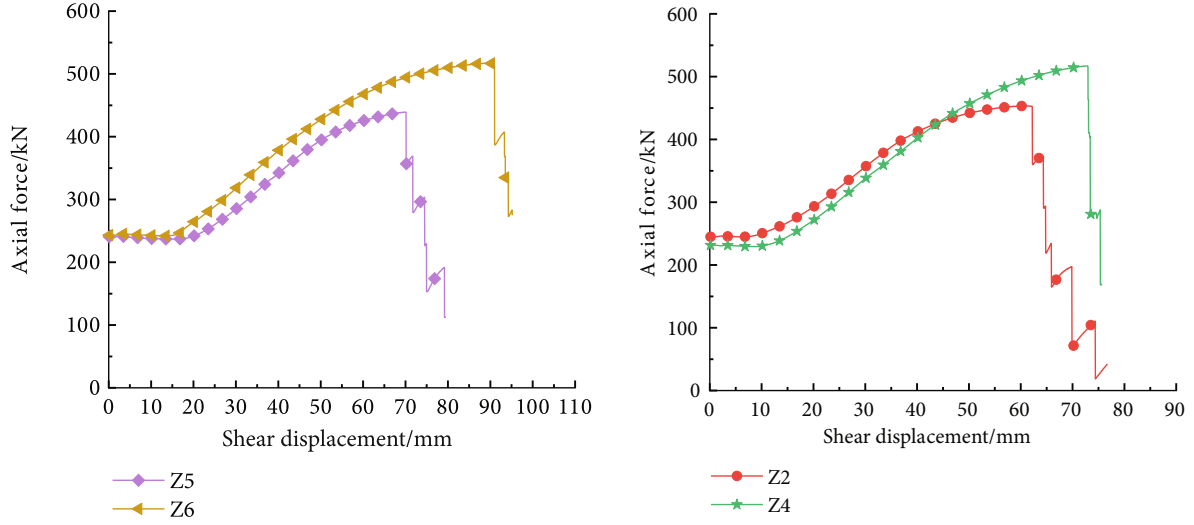
(a) Comparison of $\Phi 21.6$ mm anchor cable and $\Phi 21.8$ mm anchor cable(b) Comparison of $\Phi 21.6$ mm ACC and $\Phi 21.8$ mm ACC

FIGURE 15: Comparison of axial force difference of anchor cable structure.

surface is not affected, and the test results are reliable. For the shear box structure, the central shear box unit and the outer units that directly bear the shear force did not produce obvious deformation and cracks under the concrete crushing force, indicating that the strength and deformation of the shear box structure can meet the test requirements.

The vertical columns and horizontal bars are the important structures of the vertical shearing system and the horizontal tensile system, and the stress and deformation state of the structure during the test is observed and checked in real time. The column and crossbar did not deform significantly during and after the test. The practical application shows that the system structure meets the strength and stiffness requirements. Meanwhile, the system base and other structures have played a good supporting role.

In terms of data collection, the system successfully collected data such as shear force, axial force, and shear displacement and integrated them into the software for unified processing. According to the data, the influence of the type, structure, and pretightening force of the supporting member on the physical and mechanical properties of the supporting member is analyzed.

4.2.1. Types of Support Members. For the convenience of description, the 1×19 strands of $\Phi 21.8$ mm anchor cable are abbreviated as 21.8 mm anchor cables; the ACC composed of 1×19 strands of $\Phi 21.8$ mm anchor cables with C-shaped tubes is abbreviated as $\Phi 21.8$ mm ACC and the 1×7 strands of $\Phi 21$. The 0.8 mm anchor cable is abbreviated as 21.6 mm anchor cable, and the ACC is composed of 1×7 strands of $\Phi 21.6$ mm anchor cable with a C-shaped tube abbreviated as $\Phi 21.6$ mm ACC. This section compares the effect of two different support member types, ACC and anchor cable, on the bearing capacity.

Figure 12 compares ACC and pure anchor cable shear force-shear displacement obtained by the tensile and shear test system of the tube-cable composite structure. As shown in Figure 12, the shear displacement-shear force curves of

TABLE 5: A comparison of the axial bearing performance of supporting members.

Test group	Support type	Axial force at break (kN)	Axial bearing capacity increase percentage
A	$\Phi 21.6$ mm ACC	453.54	14.01%
	$\Phi 21.8$ mm ACC	517.06	
B	$\Phi 21.6$ mm anchor cable	439.09	17.76%
	$\Phi 21.8$ mm anchor cable	517.06	

the test group are similar, and they all experienced the friction-overcoming stage, the full contact stage, the yield stage, and the breaking stage. Before the breaking of the support member, when the shear displacement is the same, the ACC can always bear a larger shear force than the anchor cable. This phenomenon is most obvious in the full contact stage and the yield stage. During this period of time, the external C-shaped tube of the ACC is gradually closed by force, wrapping the anchor cable and forming a whole with the anchor cable, acting in synergy and bearing together. According to the test results, the maximum shear force of the joint plane anchored by $\Phi 21.6$ mm ACC is 1204.16 kN, which is about 7.4% higher than the maximum shear force of 1120.9 kN on the joint plane anchored by $\Phi 21.6$ mm pure cable. The maximum shear force of the joint surface anchored by $\Phi 21.8$ mm ACC is 1572.1 kN, which is 10.7% higher than the maximum shear force of 1419.7 kN of the joint surface anchored by $\Phi 21.8$ mm pure cable. A preliminary conclusion can be drawn from the comparison: compared with the anchor cable, the ACC anchored joint surface has better shear resistance.

The axial force data is measured by the force sensors at both ends of the specimen, with one value on the left and one on the right. Due to factors such as sensor error or

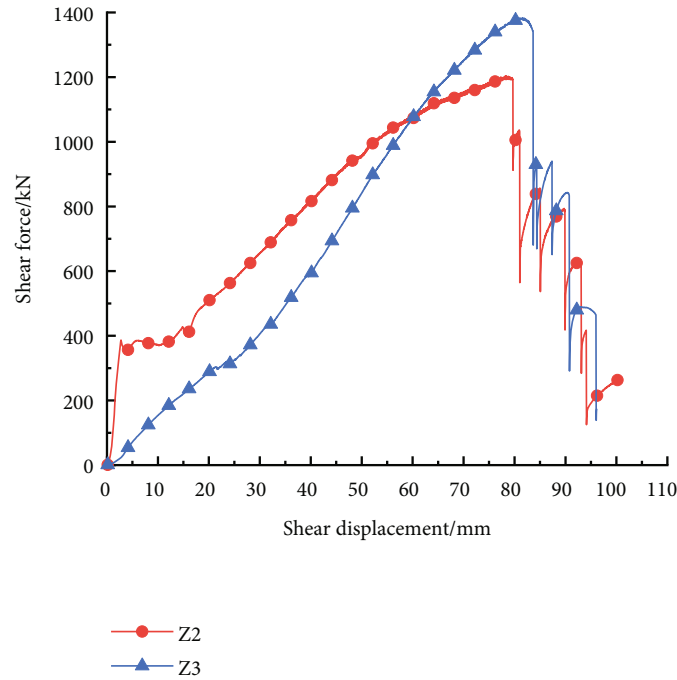


FIGURE 16: Influence of pretightening force on the shear resistance of supporting members.

friction, the left and right axial force values are not the same, but the difference is not large, and the overall trend is the same. The average value of the left and right axial forces is taken during the curve. Figure 13 shows the comparison of the axial force-shear displacement between the ACC and the pure anchor cable. As shown in Figure 13, the changing trend of the axial force-shear displacement curve of the test group is the same. The important test and calculation results are listed in Table 4.

The data in Table 4 shows that for the supporting member with a diameter of 21.6 mm, the axial bearing capacity of the ACC is significantly improved than the pure anchor cable, which is about 14.76% higher. For the 21.8 mm diameter support member, the ACC is almost the same as the pure anchor cable axial bearing capacity. ACC has no obvious effect on improving the axial bearing capacity.

4.2.2. Types of Anchor Cables. ACC is the support form of the combination of anchor cable with C-shaped tube, so the type of anchor cable has an important influence on the bearing capacity of ACC. The schematic diagram of the structure of 1×19 strands of $\Phi 21.8$ mm anchor cable and 1×7 strands of $\Phi 21.6$ mm anchor cable is shown in Figure 14.

According to the test results, the maximum shear force on the joint surface anchored by $\Phi 21.8$ mm ACC is 1572.10 kN, which is 13.7% higher than the maximum shear force of 1383.2 kN on the joint surface anchored by $\Phi 21.6$ mm ACC. Similarly, the maximum shear force on the joint surface anchored by the $\Phi 21.8$ mm anchor cable is 1419.71 kN, which is 26.7% higher than the maximum shear force of 1120.9 kN on the joint surface anchored by the $\Phi 21.6$ mm cable. The results show that the 1×19

-strand anchor cable structure has a better control effect on the shear deformation of the joint plane than the 1×7 -strand anchor cable structure when the diameters are close.

The axial force-shear displacement curves of Z5 and Z6 are shown in Figure 15. For analysis, the important test and calculation results are listed in Table 5.

The two groups of data in Table 5 show that the axial bearing capacity of the two test groups A and B has been increased to different degrees: the axial bearing capacity of $\Phi 21.8$ mm ACC is increased by about 2.61% compared with $\Phi 21.8$ mm ACC. The axial bearing capacity of the $\Phi 21.8$ mm anchor cable is increased by about 17.76% compared with the $\Phi 21.6$ mm anchor cable. In summary, the axial bearing capacity of the tube-cable composite structure will change according to the internal anchor cable structure, and the axial bearing capacity of the $\Phi 21.8$ mm anchor cable structure is greater.

4.2.3. Preload. Figure 16 is a comparison diagram of shear force-shear displacement obtained by applying different preload forces to the ACC through the tensile-shear test system of the tube-cable composite structure. As shown in Figure 16, Z2 has a straight line at the stage of overcoming the friction force at the beginning of the test. At this time, the shear force increases sharply, and the shear displacement remains almost unchanged. The blocks are pressed against each other under the action of the pretightening force. During the application of the normal force, the friction between the blocks must be overcome until the maximum static friction force is reached, and the relative slip begins to occur. Because the applied preload force of Z3 is negligible, the normal force is soon enough to overcome the friction force between the blocks after the start of the test, so the curve

of this test group increases uniformly. Meanwhile, observing the curve, we found that the preload applied to the ACC will cause the ACC to enter the yield stage earlier. The maximum shear force at break was compared between the two groups of tests. The maximum shear force of the test group with 10 kN applied when the ACC failed was 1383.19 kN, which was about 14.9% higher than the maximum shear force of 1204.2 kN when 250 kN of preload was applied to the ACC.

5. Conclusion

This paper elaborates the design idea of the tensile-shear test system for the combined structure of tube and cable, which is independently developed to study the tensile-shear mechanical properties of the combined structure of bolt, anchor, cable, and tube. Firstly, based on theoretical analysis, the parameters of the system are calculated, and then, the dimensions of the frame columns and cross bars of the main structure of the system and the wall thickness of the shear box are designed through numerical simulation. Finally, multiple sets of tests verify the structural stability, functional practicability, and reliability of the cable (rod) tensile-shear test system. The main research conclusions are as follows:

- (1) The new tensile-shear test system for combined structure of tubes and cables has the following advantages: (1) the maximum displacement of the shearing system is set to 250 mm to ensure that the supporting members can be sheared and the equipment has sufficient loading space. (2) Tensile test and double shear test in two modes can be carried out. In addition to the double shear test of a composite load of compressive shear on the shear plane, the friction between concrete can also be eliminated by pulling the supporting member through the lock. A pure shear double shear test was performed. (3) Correct the size of the shear box, and set a 5 mm gap between the shear boxes to effectively avoid the test error caused by the shear box to the block shearing.
- (2) Through theoretical calculation, the design value of the maximum test load of the horizontal loading system is 1200 kN, the design value of the maximum test displacement of the horizontal loading system is 200 mm, and the design value of the maximum test load of the vertical loading system is 6000 kN.
- (3) According to the simulation results, the thickness of the shear box steel plate is determined to be 20 mm. At this time, the maximum strain of the shear box is about 2.7‰, less than 3‰, and the maximum stress is about 450.94 MPa, which is less than the yield strength. The diameter of the vertical loading reaction frame column is 220 mm, the maximum deformation of the vertical frame is about 0.52 mm, the strain is about 0.17‰, and the maximum stress is about 190.79 MPa. The diameter of the crossbar of the horizontal loading reaction frame is 80 mm, the maximum deformation of the horizontal frame is about 0.19 mm, the strain is about 0.06‰, and the

maximum stress is about 275.85 MPa. The deformation and strength of the three main structures meet the requirements

- (4) The field application shows that the research and development of the tensile and shear test system for the combined structure of the tube and cable meet the expected design requirements. During the test, the concrete and the supporting members were subjected to shear force, and the shear plane was always located between the gaps of the shear box, and the shear box did not affect the test results. The support members were sheared, the test was over, and the main mechanical structure of the test system was not significantly deformed. The double shear test was successfully completed, and the test data such as shear force, shear displacement, and axial force were successfully obtained through the sensor.
- (5) We found that ACC has more outstanding shear resistance than ordinary anchor cables. The structure of wrapping a layer of C-shaped tube outside the anchor cable can effectively improve the maximum shear force when the support member breaks. However, this structure improves the axial bearing capacity of the support member. However, its improvement effect is not obvious. The test shows that the anchor cable structure with a diameter of 21.8 mm has stronger shear resistance and can also effectively improve the axial bearing capacity.

Data Availability

The data used to support the findings of this study are included within the article.

Conflicts of Interest

The authors declare no conflict of interest.

Acknowledgments

This research described in this paper was financially supported by the National Natural Science Foundation of China-Research (No. 51474218).

References

- [1] W. Ji-yu, W. Fang-tian, and Z. Xi-gui, "Stress evolution mechanism and control technology for reversing mining and excavation under mining-induced dynamic pressure in deep mine," *Geofluids*, vol. 2022, Article ID 4133529, 17 pages, 2022.
- [2] G.-f. Wang and Y.-h. Pang, "Surrounding rock control theory and longwall mining technology innovation," *International Journal of Coal Science & Technology*, vol. 4, no. 4, pp. 301–309, 2017.
- [3] W.-b. Xie, S.-g. Jing, Y.-k. Ren, and T. Wang, "The invalidation mechanism of bolt-mesh support in soft coal roadway," *Procedia Earth and Planetary Science*, vol. 1, no. 1, pp. 384–389, 2009.

- [4] D.-d. Chen, C.-w. Ji, S.-r. Xie et al., "Deviatoric stress evolution laws and control in surrounding rock of soft coal and soft roof roadway under intense mining conditions," *Advances in Materials Science and Engineering*, vol. 2020, Article ID 5036092, 18 pages, 2020.
- [5] H. P. Kang, "Seventy years development and prospects of strata control technologies for coal mine roadways in China," *Chinese Journal of Rock Mechanics and Engineering*, vol. 40, no. 1, pp. 1–30, 2021.
- [6] H.-p. Kang, J.-h. Yang, and X.-z. Meng, "Tests and analysis of mechanical behaviours of rock bolt components for China's coal mine roadways," *Journal of Rock Mechanics and Geotechnical Engineering*, vol. 7, no. 1, pp. 14–26, 2015.
- [7] H.-p. Kang, "Support technologies for deep and complex roadways in underground coal mines: a review," *International Journal of Coal Science & Technology*, vol. 1, no. 3, pp. 261–277, 2014.
- [8] L. Yan, M. Chao, Z. Lian-ying, and L. Bing, "Influence research for softening and swelling of weakly cemented soft rock on the stability of surrounding rock in roadway," *Geofluids*, vol. 2022, Article ID 6439277, 12 pages, 2022.
- [9] S. Krzysztow, Z. Krzysztow, Z. Anna, D. B. Apel, X. Wang Jun, and G. L. Huawei, "Choice of the arch yielding support for the preparatory roadway located near the fault," *Energies*, vol. 15, no. 10, p. 3774, 2022.
- [10] R. L. Shan, Y. H. Peng, X. S. Kong et al., "Research progress of coal roadway support technology at home and abroad," *Chinese Journal of Rock Mechanics and Engineering*, vol. 38, no. 12, pp. 2377–2403, 2019.
- [11] R. Shan, X. Tong, P. Huang et al., "Research on the anchor cable combined with the c-shaped tube and the mechanical properties," *Rock and Soil Mechanics*, vol. 43, no. 3, pp. 602–614, 2022.
- [12] R.-l. Shan, B. Yong-sheng, H. Peng-cheng, L. Wei-jun, L. Geng-zhao, and L. Zhi-xiong, "Study on double-shear test of anchor cable and C-shaped tube," *Shock and Vibration*, vol. 2021, Article ID 9948424, 10 pages, 2021.
- [13] S. Huang, X. Meng, G. Zhao et al., "Research and performance test of new full-length anchorage material," *Advances in Materials Science and Engineering*, vol. 2021, Article ID 9937751, 11 pages, 2021.
- [14] S. Krzysztow, "An experimental investigation into the stress-strain characteristic under static and quasi-static loading for partially embedded rock bolts," *Energies*, vol. 14, no. 5, p. 1483, 2021.
- [15] T. Zhigang, L. Mengnan, P. Shihui, G. Ming, and H. Manchao, "Research on mechanical property and engineering application of cable with high constant resistance and large deformation," *Journal Of Mining Science And Technology*, vol. 5, no. 1, pp. 34–44, 2020.
- [16] M. He, Z. Tao, and B. Zhang, "Application of remote monitoring technology in landslides in the Luoshan mining area," *Mining Science and Technology*, vol. 19, no. 5, pp. 609–614, 2009.
- [17] R. S. Yang, Y. L. Li, M. S. Wang et al., "Experimental study of shear mechanical properties of orestressed cable bolts," *Journal of China University of Mining and Technology*, vol. 47, no. 6, pp. 1166–1174, 2008.
- [18] H. Rasekh, N. Aziz, A. Mirza et al., "Double shear testing of cable bolts with no concrete face contacts," *Procedia Engineering*, vol. 191, pp. 1169–1177, 2017.
- [19] J. Huang, Y. Ye, W. Wang et al., "Study on tensile test and shear test of GFRP bolt on the bases of its application," *Chian Mining Magazine*, vol. 19, no. 10, pp. 94–96, 2010.
- [20] S. Meng, W. Zhang, F. Shen et al., "Experimental study on tensile and shear mechanical properties of GFRP bolt," *Guangzhou Architecture*, vol. 46, no. 5, pp. 11–14, 2018.
- [21] N. Aziz, A. Mirza, J. Nemcik, H. Rasekh, and X. Li, "A follow up to study the behavior of cable bolts in shear: experimental study and mathematical modeling," in *Coal Operator's Conference*, pp. 24–31, Wollongong, 2016.
- [22] British Standard Institution, "Strata reinforcement support system components in coal mines, specification for flexible systems for roof reinforcement," 2009.
- [23] B. Ludvig and L. Di, "Shear test of anchor rod," *Renming Changjiang*, vol. 4, pp. 51–58, 1987.
- [24] Z. Wei and L. Quan-sheng, "Analysis of deformation performance of pre-tensioned bolt based on shear test," *Rock and Soil Mechanics*, vol. 35, no. 8, pp. 2231–2240, 2014.
- [25] N. Aziz, D. Pratt, and R. Williams, "Double shear testing of bolts," in *Coal Operators Conference*, Wollongong, NSW, Australia, 2003.
- [26] Y. A. N. G. Guanyu, *Study on the Behaviors and Failure Characteristics of Cable Bolt under Various Shearing Loading Experimental Environment*, China University of Mining and Technology, Xuzhou, 2017.
- [27] A. Mirzaghobanali, H. Rasekh, N. Aziz, G. Yang, S. Khaleghparast, and J. Nemcik, "Shear strength properties of cable bolts using a new double shear instrument, experimental study, and numerical simulation," *Tunnelling and underground space technology*, vol. 70, pp. 240–253, 2017.
- [28] M. Saadat and A. Taheri, "Effect of contributing parameters on the behaviour of a bolted rock joint subjected to combined pull-and-shear loading: a DEM approach," *Rock Mechanics and Rock Engineering*, vol. 53, no. 1, pp. 383–409, 2020.
- [29] X.-w. Li, N. Aziz, A. Mirzaghobanali, and J. Nemcik, "Behavior of fiber glass bolts, rock bolts and cable bolts in shear," *Rock Mechanics and Rock Engineering*, vol. 49, no. 7, pp. 2723–2735, 2016.
- [30] L. Li, P. C. Hagan, S. Saydam, B. Hebblewhite, and Y. Li, "Parametric study of rockbolt shear behaviour by double shear test," *Rock Mechanics and Rock Engineering*, vol. 49, no. 12, pp. 4787–4797, 2016.